Food Hydrocolloids 141 (2023) 108718

Contents lists available at ScienceDirect

Food Hydrocolloids

journal homepage: www.elsevier.com/locate/foodhyd

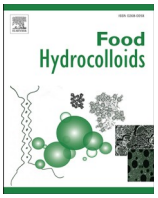

Generating slow digestibility in cooked potatoes by modulating starch accessibility to α-amylase and mucosal α-glucosidase to different levels

Andrea Gómez-Maqueo, Alvaro Ferreira-Lazarte, Nur Syahirah Amirruddin, Amy Hui-Mei Lin *

*Singapore Institute of Food and Biotechnology Innovation (SIFBI), Agency for Science, Technology and Research (A*STAR), 31 Biopolis Way, Nanos #01-02, Singapore, 138669, Republic of Singapore*

ARTICLE INFO

Keywords:
Potato
Starch digestibility
Mucosal α-glucosidase
α-amylase
Glucogenesis
Pectin
Glycemia

ABSTRACT

Health issues associated with overconsuming rapidly digestible glycemic carbohydrates continue to be prevalent globally. Transforming starch digestion from a hyperglycemic response to a sustained dietary glucose profile is an ideal digestion scenario. Digesting starch to glucose requires α-amylase (AMY) and mucosal α-glucosidase (m-AG). AMY can quickly break down starch molecules, and m-AG functions as the gatekeeper of dietary glucose production. In this study of cooked potatoes, we hypothesize that slow glucogenesis from starch can be achieved by modulating the accessibility of AMY and m-AG to starch to different levels by modifying cell wall permeability by promoting cross-linking of calcium with endogenous pectins. Raw potato cubes were blanched with 0–500 mg/L calcium solution, followed by steaming. Fully cooked potatoes with the pre-treatment had up to 41% and 99% reduction of the permeability for dextran probes of 20 kDa and 70 kDa, respectively, and a non-detectable permeability of 150 kDa dextran. Permeability data indicated a decrease in the accessibility of AMY and a complete restriction of m-AG to access starch in cells supported by data on starch susceptibility to both AMY and m-AG separately. In vitro stimulated gastrointestinal digestion data demonstrated a blunt glucose profile with a reduction of RDS from 80% to 46% and an increase of SDS from 12% to 37%. By modulating starch accessibility to AMY and m-AG to different extents, cooked potatoes were fully digested with a slow glucose-released profile. The modification was a pre-treatment, and modified potatoes can be processed into potato foods, such as french fries, mashed potatoes, and others.

1. Introduction

The overconsumption of rapidly digestible glycemic carbohydrates is associated with increased risks of developing type 2 diabetes, obesity, and other metabolic disorders, and it continues to be a prevalent societal problem. Removing carbohydrates from daily meals decreases energy supply and may quickly reduce body weight, primarily caused by diuresis associated with active gluconeogenesis and the consequent change in liver and muscle weight (Bray, 2003). However, the long-term efficacy of low-carbohydrate diets in weight loss and metabolic benefits was not optimistic (Barber, Hanson, Kabisch, Pfeiffer, & Weickert, 2021). Some low-carbohydrate diets substitute the caloric energy source with high-protein and high-fat foods. Such a combination can cause some health risks, such as fatigue (Winwood-Smith, Franklin, & White, 2017), osteoporosis associated with ketosis, inflammation from an increased dietary saturated fat intake, dysbiosis caused by the imbalanced consumption of fats, proteins, and fiber, and micronutrient deficiencies (Barber et al., 2021). Starch is the primary glycemic carbohydrate, and dietary glucose, the digestion product of starch, is a critical caloric nutrient. In addition to providing dietary glucose, carbohydrate foods offer non-starch macronutrients, including proteins, and micronutrients, such as minerals and vitamins. Fiber is another critical component in carbohydrate foods, and a significant reduction of fiber intake can lead to severe adverse impacts on gut health (Barber et al., 2021). Beyond the nutritional functionality, carbohydrates are also essential in forming food structures due to their broad technical functionalities (i.e., viscosity). Carbohydrates also create desirable sensory attributes through reactions, such as caramelization or the Maillard reaction. However, despite the beneficial attributes of starch, balancing the supply of caloric energy and nutrients and the prevalence of health risks continues to be a dilemma of starchy food consumption.

The nutritional quality of starchy foods is closely associated with the rate of starch digestion and blood glucose excursions, whether it is comprised of rapidly digestible starch (RDS) or slowly digestible starch

* Corresponding author.
E-mail address: amy_lin@sifbi.a-star.edu.sg (A.H.-M. Lin).

https://doi.org/10.1016/j.foodhyd.2023.108718
Received 30 October 2022; Received in revised form 20 March 2023; Accepted 21 March 2023
Available online 22 March 2023

(SDS), and it is evaluated through concepts such as the glycemic index. Nevertheless, research has shown that the impact of dietary glucose generation goes beyond the initial rate of glucose released from starch, which is reflected in the rise of blood sugar. Research in the ileal perfusion of carbohydrates identified a correlation between slow starch digestion and slow gastric emptying of carbohydrates (Jain et al., 1989). Dietary glucose released in the ileum has also been shown to stimulate the release of hormones (i.e., GLP-1) and peptide tyrosine-tyrosine (PYY), which promotes the ileal brake effects (Maljaars, Peters, Mela, & Masclee, 2008; Schirra & Goke, 2005; Siegle, Schmid, & Ehrlein, 1990; Spiller et al., 1988). The ileal brake is inhibitory feedback that controls the transit of a meal into the gastrointestinal tract, which helps to optimize digestion and the absorption of nutrients. Recent research findings further demonstrated the benefits of distal digestion of starch into the ileum to reduce food intake and weight gain through the gut-brain axis response (Lim, Ferruzzi, & Hamaker, 2021). Scientifically, research is approaching the goal of managing postprandial glycemic response through a dietary approach. However, starchy foods in modern diets are often rapidly digested that cannot reach the ileum before it is converted to dietary glucose. A very slow digestibility to supply moderate and sustained dietary glucose is necessary to regulate starch nutritional quality. Attaining such quality is expected to improve physiological responses leading to better food intake and body weight management in the long term (Lim et al., 2021).

Digesting starch into absorbable glucose in humans requires both α-amylase (AMY) and mucosal α-glucosidase (m-AG), which consists of N- and C- terminal subunits of maltase-glucoamylase (MGAM) and sucrase-isomaltase (SI) (Lin, Lee, & Chang, 2016). Each enzyme plays a unique role in starch digestion, which involves the breakdown of large starch polymers and the generation of glucose. AMY and m-AG degrade starch polymers with different hydrolytic mechanisms. AMY, an endo-hydrolytic enzyme, progressively breaks down starch polymers from half a million or more glucosyl units into oligomers (i.e., maltose, maltotriose, α-limit dextrin). Despite contributing to the quick degradation of starch polymers, AMY does not produce a significant quantity of glucose. M-AG, on the other hand, is the glucose generator. M-AG directly digests large starch polymers into glucose and converts AMY-hydrolysates into glucose (Lin, Hamaker, & Nichols, 2012; Lin, Nichols, et al., 2012). Generating sufficient dietary glucose requires the glucogenic activity of m-AG. In this sense, for m-AG to slowly release dietary glucose, we controlled the generation of the primary substrates (i.e., AMY hydrolysates) of m-AG in this study. We hypothesize that dietary glucose can be slowly released from cooked starchy foods by modulating the hydrolytic capacity of AMY and m-AG.

Potatoes, a staple starchy food, are essential to food security and poverty eradication as the most critical non-cereal food in the world (Food and Agriculture Organization of the United Nations, 2009). Potatoes provide essential caloric energy. Additionally, potatoes provide protein, dietary fiber, and micronutrients, such as vitamins C and B6, thiamine, niacin, folate, magnesium, and antioxidants (Wijesinha--Bettoni & Mouillé, 2019). Although potatoes have gained a reputation as a cause of hyperglycemic-related health risks (Muraki et al., 2016; Quan et al., 2022), many factors contribute to the nutritional characteristics of the potato. Potato starch consists of resistant starch as well as rapidly digestible starch, depending on the processing techniques (Kingman & Englyst, 1994; Mishra, Monro, & Hedderley, 2008). Raw starch (native starch) in potatoes has a low susceptibility to starch degradation enzymes (Jane, 2006). Processing (i.e., cooking) solubilizes granular starch and increases starch digestibility resulting in a high postprandial glycemic response (Kingman and Englyst, 1994). Genetic factors further broaden the diversity of potato's functional and nutritional properties (Pinhero et al., 2016). The maturity level of potato tubers and storage conditions can also directly impact digestion (Jansky & Fajardo, 2016; Lal et al., 2021). Therefore, the glycemic index of cooked potatoes has a broad range between 23 and 144 (Foster-Powell, Holt, & Brand-Miller, 2002).

Each crop has a different microstructure. In potato tubers, starch granules are located in the parenchyma cells, separating them from other molecules (e.g., proteins) (Fig. 1A). Preliminary studies showed parenchyma cells remained intact after potatoes were processed into french fries (Fig. 1B). These results indicate that potato starch is digested into glucose only when starch degradation enzymes can enter parenchyma cells. Research shows potato cell walls have a high permeability, which enables starch to be digested quickly after interacting with intestinal fluids (Ding et al., 2021; Do, Singh, Oey, & Singh, 2020). Potato cell walls comprise 70% non-cellulosic polysaccharides forming a gel-like matrix phase with microfibrillar phase of cellulose (Harris, 2009). Microfibrils are 4–6 nm in some crops with similar cell structures in potatoes, such as onion (*Allium cepa*) and mouse-ear cress (*Arabidopsis thaliana*) (Harris, 2009). The gel-like matrix phase is primarily formed by pectic polysaccharides (pectin, ~56% of total polysaccharides of cell walls), usually composed of four domains: homogalacturonan (HG), rhamnogalacturonan I, rhamnogalacturonan II, and xylogalacturonan. HG domain is known as "smooth" regions comprised of linear chains of α-1,4-D-galacturonic acid residues, where some residues are methyl esterified at the C-6 position. The de-esterified galacturonic acid residues can cross-link and form gels by forming an "egg-box" junction zone via calcium (Jarvis, 1984). Therefore, we hypothesize that the permeability of cell walls can be modified by promoting cross-linking and forming a gel-like structure. Our approach was to apply a blanching treatment with calcium. Through the chelation of calcium ions with endogenous potato pectin, we expect to manipulate the accessibility of starch to AMY (starch degradation enzyme) and m-AG (starch

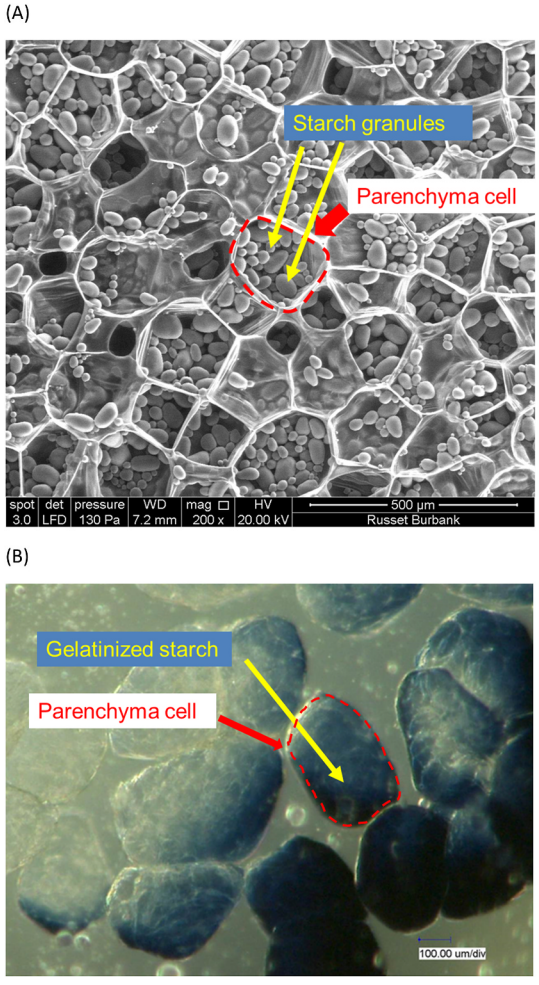

Fig. 1. Morphology of the microstructure of an un-cooked potato tuber (A) and cooked potatoes (french fries) (B), in which starch is in navy blue.

degradation and glucose generation enzyme) and further modulate the dietary glucose generation from starch.

2. Materials and methods

2.1. Materials

Potato (*Solanum tuberosum* L. Mill.) tubers of the Russet Burbank cultivar were commercially planted in Idaho (U.S.A.) and obtained from a local supermarket (NTUC FairPrice, Singapore). Tubers were selected based on firmness, skin finish, and absence of bruises, cuts, and discoloration. Ten potato tubers were used to examine tuber size, moisture content, and starch content. The average tuber weight (190.8 ± 11.2 g), length (9.5 ± 0.2 cm), and width (5.6 ± 0.4 cm) were determined using a ruler and a balance. The average moisture content (83.5 ± 1.6% wet basis) was determined by drying in an oven at 60 °C for 24 h, in triplicate. Total starch content (79.7 ± 0.7% dry basis) was measured in triplicate following the AOAC Method 996.11 and AACC Method 76–13.01 (AOAC International, 2005).

Ultrapure water was obtained from a water purification system (Mili-Q® IQ, Merck KGaA, Darmstadt, Germany). AMY enzymes from porcine pancreas, pepsin from porcine gastric mucosa, pancreatin from porcine pancreas, amyloglucosidase from *Aspergillus niger*, invertase from baker's yeast *S. cerevisiae,* and rat intestinal acetone powder (RIAP) were from Sigma-Aldrich (St. Louis, MO) through Merck KGaA (Darmstadt, Germany). Merck KGaA also supplied calcium chloride, calcium chloride dihydrate, sodium chloride, glycerol, hydrochloric acid, sodium hydroxide, sodium azide, guar gum, sodium acetate, maltose, glucose, the fluorescein isothiocyanate (FITC)- dextrans, and Amicon® Ultra centrifugal filters used in this study. A D-glucose assay kit (GOPOD format) and calcofluor white stain were obtained from Megazyme Ltd. (Wicklow, Ireland).

2.2. Potato tuber microstructure observations

2.2.1. Morphology of the microstructure of raw potato tubers

One cube (5 mm^3) was cut from the cortex section of a potato tuber. The cube was transferred into a microtube with 1 mL fixatives, which composes of 2% (v/v) paraformaldehyde and 2% (v/v) glutaraldehyde in 0.1 M phosphate buffer at pH 7.2. The microtube was microwaved at 750 W for 2 min and 30 s using a laboratory microwave processor (PELCO BioWave Pro, Ted Pelle Inc., Redding, CA). The fixative was removed and replaced with 1 mL fresh fixative and repeated with microwave heating. After the fixation, the potato cube was rinsed with deionized water three times. Before examining the sample with a scanning electron microscope (SEM), an approximately 1 mm thick slice was cut out from the cube using a double-sided razor blade and stuck to carbon tape on the SEM stub. The sample was examined directly under a low vacuum (130 Pa in the chamber) using an FEI SEM (Quanta 200 F, FEI Company, Hillsboro, OR). The spot size was 3.0, and the voltage was 20 kV during the examination.

2.2.2. Morphology of the microstructure of cooked potatoes (French fries)

The microstructure of cooked potatoes was examined by using french fries as an example. French fries made of Russet Burbank cultivar were freshly fried in a commercial setting at J.R. Simplot (Boise, ID, U.S.A) in a preliminary study. Three strips were hand-pressured with a potato masher. Then, strips were cut open by a razor blade, and a small portion (around the size of a rice grain) of the interior was transferred into a 2-mL microtube. The sample was mixed with ~1 mL diluted Lugol's solution (0.0075% v/v) with a spatula, followed by handshaking for 1 min. Three drops of the suspension were transferred onto a glass slide, overlaid with a cover slip, and examined with a light microscope (Nikon Eclipse E600, Melville, NY, U.S.A.).

2.3. Potato tuber modification

Five potato tubers were washed, peeled, and sliced into 1 cm^3 cubes for each treatment. Potato cubes were placed into a 500-mL beaker at a 1:3 ratio (w/v) of potato solution. The solution was prepared with calcium chloride at 0 (control), 100, 300, and 500 mg/L. The potato cubes and solution were placed in a beaker in a water bath at 70 °C for 30 min. After heating, the solution was discarded and replaced with a new corresponding calcium solution, in which the ratio of potato to solution was 1:6 (w/v). Potato cubes with new calcium chloride solution were placed at ambient temperature (approximately 25 °C) for 25 min. The potato cubes were removed from the solution and patted dry with paper towels before the following cooking.

Modified (pre-treated) potatoes were cooked by a commercial steamer for 35 min (Tefal VC1401, Groupe SEB, Écully, France). Steaming was selected among common cooking methods for the easiness to maintain consistent processing parameters, such as moisture content, sample size and shape, etc. Potato cubes were wrapped in aluminum foil to prevent water loss during steaming. Cooked potatoes were cooled to room temperature before further analyses, and control and treatment were cooked and cooled at the same time. The following analyses included AMY hydrolysis, m-AG digestion, in vitro simulated gastrointestinal digestion, parenchyma cell isolation for cell wall permeability assay, and texture profile analysis.

2.4. Assessing cell wall permeability by the fluorescence recovery after the photobleaching (FRAP) method

Potato parenchyma cells were isolated from the potato cubes treated with 500 mg/L calcium described in Section 2.2 following the method of Dhital, Baier, Gidley, and Stokes (2018) (Dhital et al., 2018). The permeability of potato cell walls was measured by fluorescence recovery after photobleaching (FRAP), in which the diffusion coefficient of various molecular sizes of fluorescein isothiocyanate (FITC)-dextrans was determined (Li, Gidley, & Dhital, 2019).

Potato cell suspension (490 μL) and FITC-dextran solution (10 μL, 5 mg/mL) were added into a 2-mL microtube. Samples were covered in aluminum foil and placed in a fridge (4 °C) for 16 h to achieve equilibrium of probe diffusion. Then, an aliquot (8 μL) of probe-cell suspension was transferred into a microarray glass slide and covered with a coverslip. We added a drop (2 μL) of calcofluor white solution (0.1%, w/v) to observe the integrity of the cell walls. Two tracks were set to simultaneously observe the calcofluor solution and the FITC-dextran at 405 nm and 488 nm excitation wavelengths, respectively. The emitted fluorescence was collected at 460 nm and 530 nm for calcofluor white and FITC-dextran, respectively. The experiments were performed using a confocal laser scanning microscope (FV3000RS, Olympus Corporation, Tokyo, Japan) and a Plan Neofluar 10 × /0.3 objective lens (Carl Zeiss Microscopy, LLC, NY, United States) at ambient temperature. The entire cell areas were set as bleaching areas with a polyline tool. The cell center was used to locate the center point of a circular region of interest (ROI) in which the fluorescence intensity was monitored. The ROI selected had a radius of approximately 100 μm. Bleaching was performed at 100% laser power at 488 nm with five scanning iterations. Fluorescence recovery was measured every 2 s for 3 min for 20-kDa FITC-dextran and 8 min for 70-kDa and 150-kDa FITC-dextran probes. Samples were prepared and analyzed in triplicate.

Diffusion coefficients were calculated utilizing the following equation (Kang, Day, Kenworthy, & DiBenedetto, 2012) for instantaneous bleaching where r_n is the radius of the sampling region and $T_{1/2}$ is the half-time of recovery. The half-time recovery was calculated by a logarithmic fit of the recovery curve.

$$D = 0.25\frac{r_n^2}{\tau_{\frac{1}{2}}}$$

2.5. Assessing the susceptibility of starch in cooked potatoes to AMY

Cooked (steamed) potatoes were ground with a mortar and pestle and passed through a sieve with 2 mm openings. Ground potatoes (3.5 g fresh weight) containing 500 mg starch were weighed into a 50-mL round-bottom centrifuge tube with 25 mL phosphate-buffered saline (PBS, 20 mM) containing 1 mM calcium chloride at pH 6.9. AMY enzyme solution was made by suspending 0.033 g of AMY from the porcine pancreas in 11 mL of PBS and placing it in a water bath at 37 °C for 5 min before use. Each potato sample tube was mixed with 5 mL AMY solution, and the hydrolysis was conducted in a shaking water bath at 37 °C at 150 strokes per minute for 120 min. Aliquots of 500 μL were transferred into a 1.5-mL microtube at 0 min and 5, 10, 20, 30, 60, 90, and 120 min. The hydrolysates were immediately placed in a boiling water bath for 10 min to inactivate the hydrolytic activity. The hydrolysates were centrifuged at 5000 *g* for 20 min. The reducing sugars in the supernatant were quantified by the miniaturized Somogyi-Nelson assay (Shao & Lin, 2018).

Reaction rates of AMY hydrolysis and m-AG digestion and the in vitro simulated gastrointestinal digestion following the method of Englyst et al. (1992 and 2018) were calculated by fitting the data time and products (i.e., glucose) to a first-order rate reaction, where C is the concentration of digested starch at time t, C_∞ is the digested concentration at an ultimate reaction, and k is a first-order rate constant (Goni, Garcia-Alonso, & Saura-Calixto, 1997).

$$C = C_\infty\left(1 - e^{-kt}\right)$$

This equation was first differentiated and then linearized (Butterworth, Warren, Grassby, Patel, & Ellis, 2012) using natural logarithms expressed as:

$$\ln\left(\frac{dC}{dt}\right) = \ln(C_\infty k) - kt$$

Thus, a plot of ln(dC/dt) against t is linear with a slope of k. The intercept on the y-axis equals ln(C_∞ k), and so C_∞ is calculated from the value of k obtained from the slope of the plot.

2.6. Assessing the susceptibility of starch in cooked potatoes to m-AG

2.6.1. Preparation of m-AG

m-AG was obtained from commercial rat intestinal acetone powder (RIAP). RIAP was suspended in 20 mM sodium phosphate buffer (pH 6.8) containing 0.2 mM calcium chloride and 0.02% (w/v) sodium azide at 4 °C. After continuous stirring for 24 h, the suspension was centrifuged at 17,200 *g* at 4 °C for 30 min. The supernatant was filtrated through a filter made of polyvinylidene fluoride (PVDF) with a 5 μm pore size, and the filtrate is described as filtrate I. Filtrate I was further separated into two fractions by Amicon® Ultra centrifugal filters with molecular weight cut-offs (MWCO) at 100 kDa and 10 kDa. Filtrate I (2 mL) was mixed with 2 mL PBS buffer and loaded into an Amicon® Ultra centrifugal filter with MWCO of 100 kDa followed by centrifugation at 4500 *g* at 4 °C for 30 min. The materials retained by the filter, which had a molecular size bigger than 100 kDa and was expected to contain m-AG, were mixed with an additional 4 mL PBS buffer and centrifugated again for 30 min. The material passed through the Amicon® Ultra with MWCO 100 kDa was loaded to Amicon® Ultra with MWCO of 10 kDa to remove molecules smaller than 10 kDa, such as sugars; the retained materials were expected to contain AMY. Both m-AG and AMY fractions were analyzed by SDS-polyacrylamide gel electrophoresis (SDS-PAGE), according to Laemmli (1970). Maltase activity was examined following Lin, Nichols, et al. (2012). One unit (U) was defined as the amount of enzyme that produces 1 μmol of glucose from a maltose solution in 1 min of reaction at pH 6.8 at 37 °C.

2.6.2. Digestion of the starch in cooked potatoes by m-AG

Ground cooked potatoes prepared as described in section 2.5 were weighted into 50-mL round bottom centrifuge tubes and mixed with PBS (pH 6.8) containing 0.2 mM calcium chloride and 0.02% (w/v) sodium azide to obtain a mixture with 10 mg starch per mL suspension. M-AG prepared in section 2.6.1. was added into the mixture (7U per mL of the suspension) before being placed in a water bath at 37 °C (Wiesebad WSB-18, Daihan Scientific Co., Ltd, Kangwon-do, Korea), shaking at 150 strokes per min for 3 h. Aliquots (100 μL) were transferred to microtubes at 0, 5, 10, 15, 20, 40, 60, 90, 120, and 180 min and immediately heated in a boiling water bath for 10 min to inactivate the hydrolytic activity. The hydrolysates were centrifuged at 10,000 *g* for 10 min (Microcentrifuge 5424, Eppendorf SE, Hamburg, Germany), and glucose was quantified using a D-glucose assay kit.

2.7. Assessing starch digestibility of cooked potatoes in an in vitro simulated gastrointestinal digestion model

Cooked potatoes were submitted to in vitro simulated gastrointestinal digestion according to the method of Engylst et al. (2018), with minor modifications. Mastication was simulated by grinding potato cubes with a mortar and pestle. Mashed samples were passed through a sieve with 2 mm openings. The ground potato sample (3.5 g) was weighed into a 50-mL round-bottom centrifuge tube and mixed with 5 mL of 0.5 M sodium acetate solution. Five marbles (1.5 cm in diameter) were placed into the tubes to assist with mechanical disruption. During the in vitro simulated gastrointestinal digestion, all reaction tubes were placed horizontally and parallel to the direction of movement in a shaking water bath at 37 °C. For the gastric phase simulation, pepsin solution (10 mL of 0.05 M HCl with 5 mg/mL pepsin and 5 mg/mL guar gum) was added into tubes and reacted for 30 min. For the intestinal phase simulation, AMY solution (5 mL) was added into tubes and continued reacting for another 120 min. The AMY solution consisted of 0.1 M calcium chloride solution with 1350 U pancreatic AMY, 3500 U of glucoamylase, and 200 U of invertase. The enzyme units were defined by the manufacturer. Aliquots were taken at 20- and 120-min intervals to determine RDS, SDS, and RS of cooked potatoes, which were pre-treated with 0 (control), 100, 300, and 500 mg/L calcium chloride solutions.

Additional data points were obtained from the hydrolysis of cooked potatoes and treated with the highest concentration of calcium chloride (500 mg/L) to generate hydrolytic kinetic data. Aliquots (0.3 mL) were taken at intervals of 0, 5, 10, 15, 20, 40, 60, 80, and 120 min, deactivated by heating in a boiling water bath for 10 min and then followed by centrifuge at 5000 *g* for 20 min. The glucose amount in the supernatant was then quantified using a D-glucose assay kit. Glucose standard (1 mg/mL) and normal maize starch (Ingredion Incorporated, Bridgewater Township, NJ) were applied to each in vitro analysis to validate data reproducibility. Each sample was analyzed in triplicate. RDS, SDS, and RS content were calculated according to the method of Englyst et al. (1992).

2.8. Examining the tuber texture profile of cooked potatoes using a texture analyzer

The texture of cooked potato cubes was examined using a TA.HDi Texture Analyzer (Stable Micro Systems Ltd, Godalming, United Kingdom) with a 30 kg N load cell. A cylinder probe with 10 mm diameter was used to penetrate a 5 cm^3 potato cube. We adopted the application program provided by Texture Expert for Windows™ (Stable Micro System, Godalming, United Kingdom). The experimental conditions were set at pre-test speed (1 mm/s), test speed (5 mm/s), post-test speed (5 mm/s), target mode (strain), strain (50%), timer (5 s), trigger type (auto/force), trigger force (5 g), and tare mode (auto). The textural parameters generated from the texture profile analysis curve were calculated by Texture Expert for Windows™ software. Five replicates of each sample were analyzed.

2.9. Statistical analysis

Statistical analyses were conducted using IBM SPSS for Windows (version 23.0, Armonk, United States), and the *t*-Student test was used for statistical pairwise comparison. Each sample was analyzed in triplicate and expressed as $M \pm SD$. Multivariate ANOVA was used to compare the dose-response data sets. In multivariate ANOVA, statistically significant differences between groups were assessed at $p < .05$ with the post-hoc statistical test Tukey-*b*.

3. Results

3.1. Cell wall permeability by the FRAP method

The control and treatment samples were steamed to examine the permeability of parenchyma cells in cooked potatoes. Data were determined via the diffusion coefficient (DC) of FITC-dextrans (Fig. 2) with a hydrodynamic radius ranging from 3 to 9 nm. The treatment decreased the DC of 20-kDa-dextran (3.24 nm) from ($M = 27.30$, $SD = 1.55$) to ($M = 16.18$, $SD = 1.17$), where $t\,(1) = 2.02$, and $p = .05$, which suggests a reduction of accessibility of small molecules entering or leaching out of parenchymal cells. The DC of 70-KDa-dextran (6.49 nm) was decreased by the treatment from ($M = 18.26$, $SD = 2.15$) to ($M = 0.02$, $SD = 0.00$), where $t\,(1) = 6.03$, and $p = .05$. The permeability of 150-kDa-dextran (9 nm) was not detected, which indicates large molecules cannot enter parenchyma cells.

3.2. The susceptibility of starch in cooked potatoes to AMY

The AMY hydrolysis kinetics shown in Fig. 3 was plotted with time against the percent of hydrolysis, and the data were applied to the first-order equation to obtain the rate constant *k*. Control and treatment samples had reaction constant *k* of 0.083 and 0.031, respectively (Fig. 3B). Data suggest calcium treatment significantly decreases the rate of AMY hydrolysis. The C_∞ of the control and treatment was 23.83 and 23.76, respectively, which indicates substrates in the control and treatment samples were hydrolyzed to similar levels ultimately. We observed a connection between the AMY hydrolysis (Fig. 3) and the in vitro-simulated digestion (section 3.4; Fig. 6.) with a Pearson's correlation coefficient *r* of 0.9519, which indicates the reduction of AMY hydrolysis drove the rate of in-vitro gastrointestinal digestion.

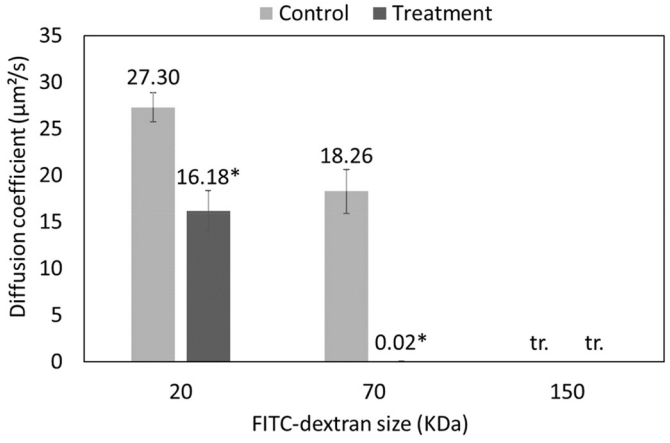

Fig. 2. Diffusion coefficients ($\mu m^2/s$) of FITC-dextrans (20 kDa, 70 kDa, 150 kDa) entered potato cells isolated from steamed potatoes without (control) and with modification (treatment with 500 mg/L calcium solution). The asterisk indicates statistically significant differences ($p < .05$) between the control and treatment samples with the same size as the FITC-dextran probe.

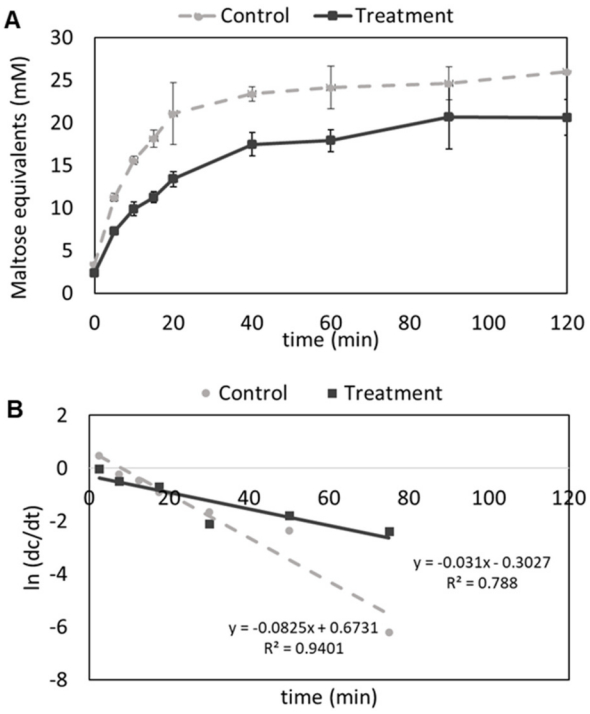

Fig. 3. In vitro AMY hydrolysis of steamed potatoes without (control) and with modification (treatment with 500 mg/L calcium solution) starch hydrolysis (A) and the logarithm of slope (LOS) plots (B).

3.3. The susceptibility of starch in cooked potatoes to m-AG

3.3.1. Characterization of m-AG fraction

Data showed the combination of membrane filtration and Amicon® Ultra centrifugal filters successfully separated m-AG from AMY of the rat intestinal powder extract. M-AG fraction, which refers to the fraction with molecular size larger than 100 kDa, had significant maltase activity with $M = 34.92$ U/mL, $SD = 2.43$. AMY fraction is referred to the fraction with molecular sizes between 10 kDa and 100 kDa, which had little activity towards maltose with $M = 0.12$ U/mL, $SD = 0.02$. Results of SDS-PAGE analysis are shown in Fig. 4. M-AG fraction was free of AMY with a lack of the 50 kDa band corresponding to AMY. A band

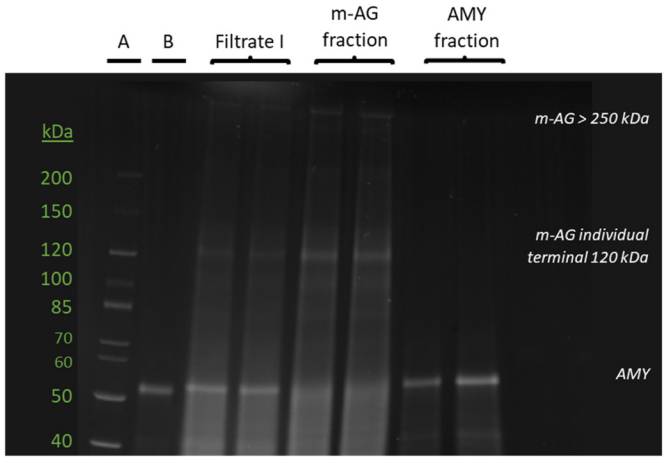

Fig. 4. SDS-PAGE analysis of m-AG and AMY fractions separated from RIAP extract. Lane A shows bands of protein markers, and lane B shows the band corresponding to porcine pancreatic AMY. Filtrate I refers to RIAP extract with a filtration with a 5 μm pore size. m-AG fraction with molecule sizes over 100 kDa; AMY fraction with molecule sizes between 10 kDa and 100 kDa.

corresponding to the size of 120 kDa was observed in the m-AG fraction, suggesting the presence of the individual terminal domain fragments of m-AG, such as C-terminal MGAM. A band presenting a size over 250 kDa was also observed, which suggests the protein complexes of MGAM and SI in the m-AG fraction. This study did not further characterize the individual protein complex; instead, maltase, which is the dominant hydrolytic activity of m-AG, was highlighted.

3.3.2. Glucogenesis from starch in cooked potatoes by m-AG

The m-AG digestion kinetics shown in Fig. 5. was plotted with time against the released glucose amount from cooked potatoes containing 10 mg starch. M-AG released approximately 27.9% of glucose from starch in the control sample while only 15% from treatment during the hydrolysis period. Data were applied to fit into a first-order equation, and C_∞ values of control and treatment samples were 5.90 and 1.57, respectively, which led to estimated starch digestion at 53.06% and 14.10% of control and treatment samples, respectively, when reaching ultimate digestion. The calculation was based on the ratio of glucose to starch multiple 0.9, in which starch amount was the C_∞ values. Results suggest that m-AG alone could substantially digest starch to glucose in the control sample, whereas the treatment samples significantly decreased glucose production.

3.4. Glucose generation rate in the in vitro simulation of starch digestibility

Both control and treatment samples were steamed to examine the influence of the treatment on cooked potatoes in an in vitro simulated gastrointestinal digestion model. The starch hydrolysis times are shown in Fig. 6A. Both control and treatment samples had two stages of digestion. The first stage reaction occurred between 0 and 20 min, followed by the second stage reaction that occurred between 20 min and 120 min. During the first stage of digestion, starch in the control potatoes was greatly hydrolyzed ($M = 80\%$, $SD = 1.4$) while only 46% ($SD = 2.3$) of starch in the treated samples was hydrolyzed, at $p \leq .05$. As a result, the treatment samples had a less pronounced slope compared to the control. During the second stage of digestion, the slope of treatment became more pronounced than that of the control. The desirable pronounced slope during the late stage of digestion demonstrates the slow digestion of starch into dietary glucose.

The glucose generation rates for each time interval (dy) are plotted against cumulative time in Fig. 6B, following the equation in Reddy and Reddy (Reddy & Reddy, 2005). In the control sample, glucose generation reached the maximum rate in 5 min, while the treatment samples reached the maximum glucose generation rate in 10 min. The maximum

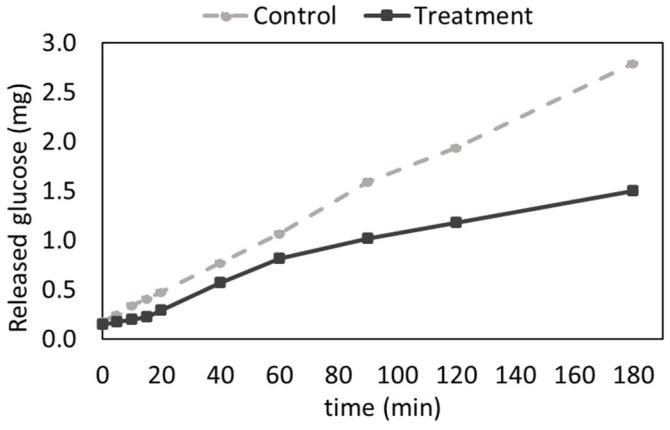

Fig. 5. In vitro starch digestion by m-AG (glucogenesis) of cooked potatoes without (control) and with modification (treatment with 500 mg/L calcium solution). Data were analyzed in triplicate, and the standard deviations were labeled in the graph though they were too small to be seen.

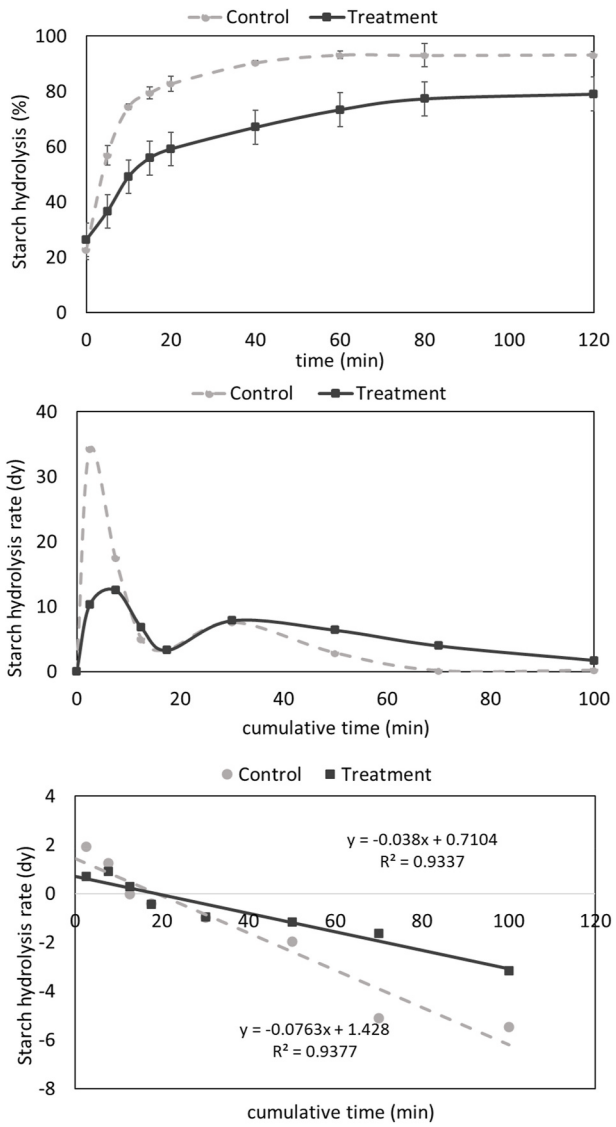

Fig. 6. In vitro simulated gastrointestinal digestion of cooked potatoes without (control) and with modification (treatment with 500 mg/L calcium solution) starch hydrolysis (A), glucose generation rate (B), and logarithm of slope (LOS) plots (C).

hydrolysis rate (% of starch hydrolysis per min) of the control and treatment was 35% and 12%, respectively. The logarithm of the slope plot is shown in Fig. 6C, in which the reaction rate (k) of the control and treatment was 0.0763 and 0.038, respectively. The control sample was completely digested and stopped releasing glucose at 70 min, while the treatment sample showed sustained glucose generation longer than 100 min.

3.5. Calcium solution dose-response on starch digestibility fractions

The RDS, SDS, and RS of cooked potatoes for both the control and treatment samples are shown in Fig. 7. The control had the highest content of RDS ($M = 80.1\%$, $SD = 1.4$). With the addition of calcium solution, RDS decreased and reached 46.4% when 500 mg/L of calcium solution was applied to the blanching. In terms of desirable SDS, treatments with 500 mg/L calcium chloride solution had the highest content $M = 36.8$, $SD = 2.2$. Although RS is not the primary interest of this study due to the lack of capacity to generate glucose, the treatment had an increase in RS compared with the control (data shown in Fig. 7).

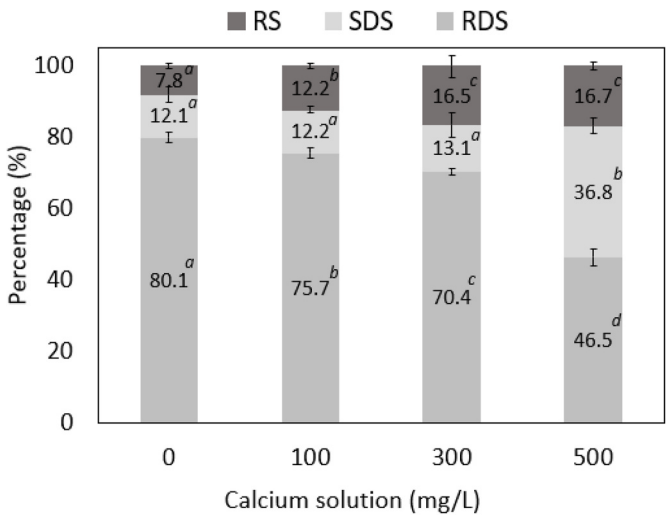

Fig. 7. Rapidly digestible starch (%), slowly digestible starch (%), and resistant starch (%) of steamed potatoes modified with calcium solution at 0 (control), 100, 300, and 500 mg/L. The letters a, b, and c were used to show statistically significant differences between variables (amount of calcium solutions) ($p < .05$).

3.6. Potato tuber texture examination by the texture profile analysis

Control and treatment samples with 500 mg/L calcium chloride were cooked and analyzed with the texture profile analysis. A double compression test was used in this study to mimic the biting action in mouths (Brandt, Skinner, & Coleman, 1963; Skinner, 2018). The hardness, adhesiveness, springiness, cohesiveness, gumminess, chewiness, and resilience are shown in Table 1. Treatment had two times higher hardness and resilience values than the control. Meanwhile, the gumminess and chewiness parameters were four times higher in the treated potatoes versus the control.

4. Discussion

In this study, the approach to modify starch digestion of cooked potatoes involved changing the permeability of cell walls to manipulate the accessibility of AMY and m-AG to starch in potato parenchyma cells. Both AMY and m-AG are critical in digesting starch into glucose. AMY has a great influence in the rate of digestion while m-AG is the primary glucose producer. M-AG can use both starch and AMY hydrolysates as substrates (Dhital, Lin, Hamaker, Gidley, & Muniandy, 2013; Lin, Nichols, et al., 2012), and m-AG alone is very capable of digesting starch to glucose. The C terminal subunit of MGAM is particularly powerful in digestion and can effectively convert ~85% of starch molecules into glucose without the pre-hydrolysis by AMY (Lin, Nichols, et al., 2012). Therefore, blocking m-AG to access intact starch molecules was critical in controlling dietary glucose generation in this study. Data on starch susceptibility to m-AG (section 3.3.2.) suggest that m-AG alone could digest starch in the control sample to ~ 53% in ultimate digestion while the modification restricted m-AG to direct digest starch and decreased C_∞ to ~14%. The modification also impacted AMY hydrolysis. Though AMY could still penetrate through cell walls in the treatment sample, susceptibility data of AMY (Fig. 3B) demonstrate a lower rate of AMY hydrolysis. An ultimate AMY hydrolysis is expected to produce substantial linear molecules, such as maltose and maltotriose, highly susceptible to m-AG. The branched form of AMY hydrolysates is also digestible by the isomaltase activity of m-AG, primarily contributed by the N-terminal subunit domain of SI. The presence of AMY amplifies m-AG digestion. However, in this study, starch must be degraded to a small size for leaching out of parenchyma cells for m-AG digestion due to the decrease of permeability (Fig. 2). A reduction of the rate of AMY hydrolysis (Fig. 3) further decreased the rate of supplying substrates to m-AG. Therefore, the outcome of the modification in this study was slow and sustained (Fig. 6B) glucogenesis from starch. The modification served as a physical barrier versus changing the conformational relationship between substrates and enzymes, broadly used when applying enzyme inhibitors to the digestion system. Therefore, we assumed the modification of cell walls did not impact the hydrolytic activity of m-AG. Data support this hypothesis that the control and treatment samples had similar glucose amounts and showed a similar area under the curves (Fig. 6B).

Table 1
Texture profile analysis of steamed potatoes previously treated in the absence (control) and presence of 500 mg/L calcium solution (treatment).

Texture parameter	Control	Treatment
Hardness (g)	4179 ± 996	8408 ± 247*
Adhesiveness (g s)	−11 ± 7	−10 ± 5
Springiness (%)	0.4 ± 0.2	0.5 ± 0.1
Cohesiveness	0.1 ± 0.0	0.1 ± 0.0
Gumminess	292 ± 38	1190 ± 215*
Chewiness	143 ± 29	563 ± 111*
Resilience	0.04 ± 0.02	0.08 ± 0.01*

Results are expressed as $M \pm SD$ (n = 3). *Indicates statistically significant differences ($p \leq .05$) between samples.

Four types of molecules participated in the digestion process: starch, AMY hydrolysates, AMY, and m-AG. The molecular size of potato starch is above 10^8 Da. The primary oligomers of AMY hydrolysates are maltose and maltotriose, which are 342 Da and 504 Da, respectively. The molecular size of maltodextrins and α-limit dextrins ranges from 6 kDa to 8 kDa with an estimated degree of polymerization (DP) at 40–60. AMY is approximately 56 kDa, and m-AG ranges from 120 kDa (individual subunits) to around 335 kDa (e.g., MGAM complex). Though the molecular size in weight does not always reflect the size of the volume, the significant difference among the four types of molecules demonstrated the potential for us to modulate the accessibility of substrates to enzymes. The permeability of FITC-dextran at 150 kDa was not detectable in both the control and treatment samples. Permeability data suggest that large molecules, such as intact starch (un-hydrolyzed starch), cannot be accessed by the enzymes located outside of parenchyma cells. The observation of cooked potatoes in the previous study (Fig. 1B) supports this statement that starch remained in cells. The modification in this study reduced approximately 40% of the permeability of FITC-dextran at 20 kDa and nearly 100% of FITC-dextran at 70 kDa. The data indicate that diffusion coefficients of AMY might be greatly decreased while m-AG might also be significantly blocked from accessing starch by modified cell walls. In this sense, the digestion of m-AG is primarily on AMY hydrolysates rather than intact starch.

The cell wall permeability was estimated by the hydrodynamic radius (R_h) of dextrans. The R_h, determined by intrinsic viscosity, at 19.5 kDa and 73.0 kDa, was 3.24 nm and 6.49 nm, respectively (Armstrong, Wenby, Meiselman, & Fisher, 2004). The minimum radius (R_{min}) of AMY is 2.54 nm, estimated based on the assumption that the protein has a spherical shape with a partial specific volume of 0.73 cm^3/g (Erickson, 2009). Therefore, the permeability of a 20-kDa-dextran probe ($R_h = 3.24$ nm) is close to the permeability of AMY ($R_{min} = 2.54$ nm), as opposed to the permeability of a 70-kDa-dextran ($R_h = 6.49$ nm). The decrease of the permeability (40%) of 20-kDa-dextran suggests a significant reduction of the permeability of AMY. Data of AMY hydrolysis rate shown in Fig. 3 support this assumption. M-AG consists of much larger molecules than AMY. M-AG is composed of MGAM and SI. Both the SI gene and the MGAM gene produce proteins with a predicted size of approximately 210 kDa. With the glycosylation of the N-linked and O-linked carbohydrates, SI is synthesized as a single polypeptide ranging from around 240 kDa–260 kDa (Moolenaar & Naim, 1995; Shapiro, Bulow, Conklin, Scheving, & Gray, 1991). Mature MGAM protein is more heavily glycosylated than SI, with a size of approximately 335 kDa

(Naim, Sterchi, & Lentze, 1988). The calculated minimum radius of MGAM is approximately 4.5 nm assuming the protein is spherically shaped. The volume size of m-AG should be much larger than 4.5 nm due to glycosylation and their molecular shape. Among the four types of molecules participating in the potato digestion process, potato starch is a giant molecule with a hydrodynamic radius ranging from 144 nm to 195 nm (Menzel, González-Martínez, Chiralt, & Vilaplana, 2019). Therefore, both potato starch and entire protein complexes of m-AG cannot pass through parenchyma cell walls. Only small amounts of the individual terminal domain of m-AG could pass through the cell walls, generating a small amount of glucose observed in this study. The measurement of molecular size, either by mass or by volume, cannot precisely determine the accessibility or leaching of molecules because the molecular size is distribution. The distinguished difference in the mass and volume size of AMY and m-AG is the key to enabling the modulation without introducing additional chemicals or enzyme inhibitors. Dose-response data demonstrate that the modification is not an unexpected reaction but strategically controlled starch degradation and glucogenesis via manipulating cell wall permeability.

Blanching is a common post-harvest processing technique. However, this technique is primarily used only for de-activating plant enzymes. In this study, glucogenesis from starch was manipulated via blanching with calcium. Calcium chloride, a GRAS chemical, was the only chemical used in this study. Calcium is typically added during blanching to enhance hardness, an ancient and safe food processing technique. In this study, the modification with calcium also increased the hardness of cooked potatoes (Table 1), which is desirable in some potato foods, such as french fries (Sadeghi, Lin, Price, Thornton, & Lin, 2021). Another molecule involved in the gelling formation is endogenous pectin. The endogenous HG is crucial for successfully manipulating digestion; however, HG is only ~20% of total pectin polysaccharides in potato cell walls (Mohnen, Bar-Peled, & Somerville, 2008). Our data demonstrated the modification resulted in a reduction of cell wall permeability. The increase of calcium concentration from 300 mg/L to 500 mg/L produced a more significant reduction of rapidly digestible starch (RDS). The permeability data of the treatment with 500 mg/L calcium demonstrated a significantly reduced permeability of 20-kDa and 70-kDa dextrans. An increase in resistant starch (RS) was also observed, and we suspect an intra-starch molecular interaction promoted by calcium resulted in the rise of RS. Research in the process also showed that further increases in calcium concentrations above 900 mg/L do not significantly reduce AMY hydrolysis (data not shown). This may be due to a limited de-esterified HG in the potato cell walls. Despite adding a small amount of calcium as a common practice to enhance AMY activity in biochemical analyses, it doesn't affect starch digestibility studies adversely. Using calcium (or other di-cations) and pectin (or other anionic polysaccharides) in developing slowly digestible starchy foods or ingredients has been a successful approach. A recent study in potato chips fortified with a mixture of vitamin C, E, calcium, sodium chloride, and surfactants demonstrated low starch hydrolysis (Duarte-Correa, Vega-Castro, López-Barón, & Singh, 2021). In the potato chip study, the digestion was carried out with milled and dehydrated samples (Duarte-Correa et al., 2021) suggesting that the microstructure strengthened by calcium is resilient to the in vitro gastrointestinal simulation.

Many modern processed (cooked) starchy foods can be rapidly digested into dietary glucose. Dietary glucose is critical caloric energy to humans, and slow digestion is expected to have many benefits toward better appetite and food intake control. This study aimed to demonstrate a way, through a simple processing technique, to offer a slow and sustained dietary glucose profile from a starchy staple food. This study strategically manipulated two critical starch degradation enzymes, AMY and m-AG, into a slow starch degradation by AMY and a complete glucogenesis by m-AG. Data on in vitro starch digestibility (Figs. 3, 5-7) showed that the modification was effective after steaming and grounding with a mortar and pestle. The results of this study suggest that the modification may have a broad application in various potato foods. Some potato foods, such as french fries, benefit from the enhanced texture attributes. Future clinical studies will validate the in vitro examination of glucogenesis and its impact on other nutritional qualities, such as improved appetite management.

Funding

This research work was supported by the Agency for Science, Technology and Research (A*STAR) under: (1) the A*STAR Central Initiatives – Food Carbohydrate Programme (Project No: C220314027), and (2) the Industry Alignment Fund – Pre-Positioning Programme Food Structure Engineering for Nutrition and Health Programme (Grant ID No: H17/01/a0/A11 & H18/01/a0/B11).

Author contributions

Andrea Gomez-Maqueo: Investigation, Methodology, Data collection, Writing- original draft; **Alvaro Ferreira-Lazarte**: Investigation, Methodology, Data collection, Writing and editing; **Nur Syahirah Amirruddin**: Data collection; **Amy H.-M. Lin**: Conceptualization, Investigation, Data curation, Supervision, Funding acquisition, Writing-review and editing.

Declaration of competing interest

None.

Data availability

The data that has been used is confidential.

Acknowledgments

We thank Yijing Shao (Univ. of Idaho, Moscow, ID, U.S.A.), Yu-Lian Lin (Univ. of Idaho, Moscow, ID, U.S.A.), and Valerie Lynch-Holm (Franceschi Microscopy and Imaging Center at Washington State Univ., Pullman, WA, U.S.A.) for preparing Fig. 1 in a preliminary study; JR Simplot (Caldwell, ID, USA) previously supporting the processing of French fries and assisting the examination shown in Fig. 1B; Shuping Lin (Research Support Centre, A*STAR, Singapore) for operating the confocal laser scanning microscope; Yee-Song Law (SIFBI, A*STAR, Singapore) for assisting protein separation.

References

AOAC International. (2005). Official methods of analysis of AOAC international. In *Starch (total) in cereal products, amyloglucosidase-α-amylase method* (18th ed. 11, pp. 75–76). Gaithersburg, Maryland, USA: Official Method 996.

Armstrong, J. K., Wenby, R. B., Meiselman, H. J., & Fisher, T. C. (2004). The hydrodynamic radii of macromolecules and their effect on red blood cell aggregation. *Biophysical Journal, 87*(6), 4259–4270.

Barber, T. M., Hanson, P., Kabisch, S., Pfeiffer, A. F., & Weickert, M. O. (2021). The low-carbohydrate diet: Short-term metabolic efficacy versus longer-term limitations. *Nutrients, 13*(4), 1187.

Brandt, M. A., Skinner, E. Z., & Coleman, J. A. (1963). Texture profile method. *Journal of Food Science, 28*(4), 404–409.

Bray, G. A. (2003). Low-carbohydrate diets and realities of weight loss. *JAMA, 289*(14), 1853–1855.

Butterworth, P. J., Warren, F. J., Grassby, T., Patel, H., & Ellis, P. R. (2012). Analysis of starch amylolysis using plots for first-order kinetics. *Carbohydrate Polymers, 87*(3), 2189–2197.

Dhital, S., Baier, S. K., Gidley, M. J., & Stokes, J. R. (2018). Microstructural properties of potato chips. *Food Structure, 16*, 17–26.

Dhital, S., Lin, A. H., Hamaker, B. R., Gidley, M. J., & Muniandy, A. (2013). Mammalian mucosal α-glucosidases coordinate with α-amylase in the initial starch hydrolysis stage to have a role in starch digestion beyond glucogenesis. *PLoS One, 8*(4), Article e62546.

Duarte-Correa, Y., Vega-Castro, O., López-Barón, N., & Singh, J. (2021). Fortifying compounds reduce starch hydrolysis of potato chips during gastro-small intestinal digestion in vitro. *Starch Staerke, 73*(9–10), Article 2000196.

Erickson, H. P. (2009). Size and shape of protein molecules at the nanometer level determined by sedimentation, gel filtration, and electron microscopy. *Biological Procedures Online, 11*, 32–51.
Goni, I., Garcia-Alonso, A., & Saura-Calixto, F. (1997). A starch hydrolysis procedure to estimate glycemic index. *Nutrition Research, 17*(3), 427–437.
Harris, P. J. (2009). Cell-wall polysaccharides of potatoes. *Advances in Potato Chemistry and Technology*, 63–81.
Jain, N. K., Boivin, M., Zinsmeister, A. R., Brown, M. L., Malagelada, J. R., & DiMagno, E. P. (1989). Effect of ileal perfusion of carbohydrates and amylase inhibitor on gastrointestinal hormones and emptying. *Gastroenterology, 96*(2 Pt 1), 377–387.
Jane, J.-l. (2006). Current understanding on starch granule structures. *Journal of Applied Glycoscience, 53*(3), 205–213.
Jansky, S., & Fajardo, D. (2016). Amylose content decreases during tuber development in potato. *Journal of the Science of Food and Agriculture, 96*(13), 4560–4564.
Kang, M., Day, C. A., Kenworthy, A. K., & DiBenedetto, E. (2012). Simplified equation to extract diffusion coefficients from confocal FRAP data. *Traffic, 13*(12), 1589–1600.
Kingman, S. M., & Englyst, H. N. (1994). The influence of food preparation methods on the in-vitro digestibility of starch in potatoes. *Food Chemistry, 49*(2), 181–186.
Lal, M. K., Kumar, A., Raigond, P., Dutt, S., Changan, S. S., Chourasia, K. N., et al. (2021). Impact of starch storage condition on glycemic index and resistant starch of cooked potato (Solanum tuberosum) tubers. *Starch - Stärke, 73*(1–2), Article 1900281.
Li, H., Gidley, M. J., & Dhital, S. (2019). Wall porosity in isolated cells from food plants: Implications for nutritional functionality. *Food Chemistry, 279*, 416–425.
Lim, J., Ferruzzi, M. G., & Hamaker, B. R. (2021). Dietary starch is weight reducing when distally digested in the small intestine. *Carbohydrate Polymers, 273*, Article 118599.
Lin, A. H.-M., Hamaker, B. R., & Nichols, B. L., Jr. (2012). Direct starch digestion by sucrase-isomaltase and maltase-glucoamylase. *Journal of Pediatric Gastroenterology and Nutrition, 55*(Suppl 2), S43–S45.
Lin, A. H. M., Lee, B. H., & Chang, W. J. (2016). Small intestine mucosal a-glucosidase: A missing feature of in vitro starch digestibility. *Food Hydrocolloids, 53*, 163–171.
Lin, A. H.-M., Nichols, B. L., Quezada-Calvillo, R., Avery, S. E., Sim, L., Rose, D. R., et al. (2012). Unexpected high digestion rate of cooked starch by the Ct-maltase-glucoamylase small intestine mucosal α-glucosidase subunit. *PLoS One, 7*(5), Article e35473.
Maljaars, P. W., Peters, H. P., Mela, D. J., & Masclee, A. A. (2008). Ileal brake: a sensible food target for appetite control. A review. *Physiology & Behavior, 95*(3), 271–281.
Menzel, C., González-Martínez, C., Chiralt, A., & Vilaplana, F. (2019). Antioxidant starch films containing sunflower hull extracts. *Carbohydrate Polymers, 214*, 142–151.
Mishra, S., Monro, J., & Hedderley, D. (2008). Effect of processing on slowly digestible starch and resistant starch in potato. *Starch Staerke, 60*(9), 500–507.
Mohnen, D., Bar-Peled, M., & Somerville, C. (2008). Cell wall polysaccharide synthesis. In M. E. Himmel (Ed.), *Biomass recalcitrance: Deconstructing the plant cell wall for bioenergy* (pp. 94–187). Oxford: Blackwell Publishing.
Moolenaar, C. E., & Naim, H. Y. (1995). Cloning and expression of human intestinal sucrase-isomaltase. *Biochemical Society Transactions, 23*(2), 304s.
Muraki, I., Rimm, E. B., Willett, W. C., Manson, J. E., Hu, F. B., & Sun, Q. (2016). Potato consumption and risk of type 2 diabetes: Results from three prospective cohort studies. *Diabetes Care, 39*(3), 376–384.
Naim, H. Y., Sterchi, E. E., & Lentze, M. J. (1988). Structure, biosynthesis, and glycosylation of human small intestinal maltase-glucoamylase. *Journal of Biological Chemistry, 263*(36), 19709–19717.
Pinhero, R. G., Waduge, R. N., Liu, Q., Sullivan, J. A., Tsao, R., Bizimungu, B., et al. (2016). Evaluation of nutritional profiles of starch and dry matter from early potato varieties and its estimated glycemic impact. *Food Chemistry, 203*, 356–366.
Quan, W., Jiao, Y., Xue, C., Li, Y., Wang, Z., Zeng, M., et al. (2022). Processed potatoes intake and risk of type 2 diabetes: A systematic review and meta-analysis of nine prospective cohort studies. *Critical Reviews in Food Science and Nutrition, 62*(5), 1417–1425.
Sadeghi, R., Lin, Y., Price, W. J., Thornton, M., & Lin, A. H.-M. (2021). *Instrumental indicators of desirable texture attributes of French fries*. LWT Food Science and Technology, Article 110968.
Schirra, J., & Goke, B. (2005). The physiological role of GLP-1 in human: Incretin, ileal brake or more? *Regulatory Peptides, 128*(2), 109–115.
Shao, Y., & Lin, A. H.-M. (2018). Improvement in the quantification of reducing sugars by miniaturizing the Somogyi-Nelson assay using a microtiter plate. *Food Chemistry, 240*, 898–903.
Shapiro, G. L., Bulow, S. D., Conklin, K. A., Scheving, L. A., & Gray, G. M. (1991). Postinsertional processing of sucrase-α-dextrinase precursor to authentic subunits: Multiple step cleavage by trypsin. *American Journal of Physiology, 261*(5 Pt 1), G847–G857.
Siegle, M. L., Schmid, H. R., & Ehrlein, H. J. (1990). Effects of ileal infusions of nutrients on motor patterns of canine small-intestine. *American Journal of Physiology, 259*(1), G78–G85.
Skinner, E. Z. (2018). The texture profile method. In *Applied sensory analysis of foods* (pp. 89–107). Routledge.
Spiller, R. C., Trotman, I. F., Adrian, T. E., Bloom, S. R., Misiewicz, J. J., & Silk, D. B. A. (1988). Further characterization of the ileal brake reflex in man - effect of ileal infusion of partial digests of fat, protein, and starch on jejunal motility and release of neurotensin, enteroglucagon, and peptide YY. *Gut, 29*(8), 1042–1051.
Wijesinha-Bettoni, R., & Mouillé, B. (2019). The contribution of potatoes to global food security, nutrition and healthy diets. *American Journal of Potato Research, 96*(2), 139–149.
Winwood-Smith, H. S., Franklin, C. E., & White, C. R. (2017). Low-carbohydrate diet induces metabolic depression: A possible mechanism to conserve glycogen. *American Journal of Physiology - Regulatory, Integrative and Comparative Physiology, 313*(4), R347–r356.
Foster-Powell, K., Holt, S. H., & Brand-Miller, J. C. (2002). International table of glycemic index and glycemic load values: 2002. The American Journal of Clinical Nutrition, 76(1), 5-56.